

# Model independent WIMP Searches in full Simulation of the ILD Detector

Christoph Bartels<sup>1,2</sup> and Jenny List<sup>1</sup>

1- DESY

Notkestrasse 85, 22607 Hamburg - Germany

2- University of Hamburg - Institut für Experimentalphysik  
Luruper Chaussee 149, 22761 Hamburg - Germany

In this study the ILC's capabilities for detecting WIMPs and measure their properties are investigated. The signal events are detected by associated production of Initial State Radiation (ISR). A model independent formulation of the signal cross section is used. The cross section is normalized by inference from the observed abundance of cosmological Dark Matter (DM). The study is performed in full simulation of the ILD00 detector model. The prospects of determining the WIMP parameters individually and simultaneously are presented.

## 1 Dark Matter and WIMPs

New physics is required from both cosmology and the known shortcomings of the Standard Model (SM). The observed non-baryonic Cold Dark Matter (CDM) density in the universe can be accounted for by introduction of a new neutral particle, stable by virtue of a new conserved quantum number. Given interactions of weak strength and masses in the range of 0.1–1 TeV these generic WIMPs naturally give the observed DM density as a thermal relic of the expansion of the early universe. Several extensions of the SM include such a WIMP candidate, e. g. SUSY with conserved R-Parity, where the LSP often is either the lightest neutralino  $\tilde{\chi}_1^0$  or the gravitino  $\tilde{G}$ . Direct WIMP pair production  $e^+e^- \rightarrow \chi\chi$  should be possible at the International Linear Collider (ILC) [1] for WIMP masses of less than half the CMS energy,  $M_\chi \leq \sqrt{s}/2$ . However, since WIMP interactions are only of weak strength, such events would be unobservable as long as no other detectable particle is associated with the pair production process. ISR provides such a detectable particle. A single photon radiated off the initial state delivers a clean signal, while the properties of the photon spectrum give information on the DM candidate. This detection channel does not only give additional information on

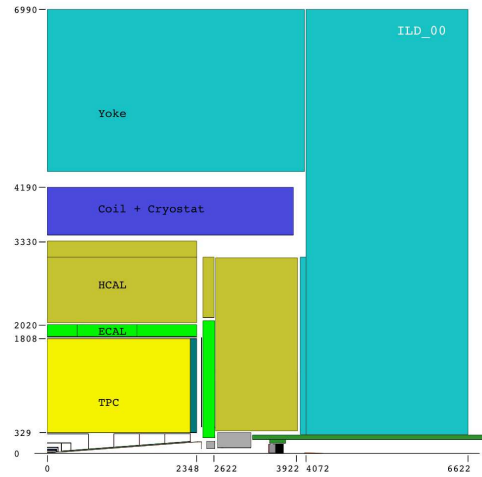


Figure 1: Quadrant of the ILD detector. Starting from the origin of the coordinate system the Time Projection Chamber (yellow) and the calorimetric system of ECAL (green) and HCAL (ocher) are shown.

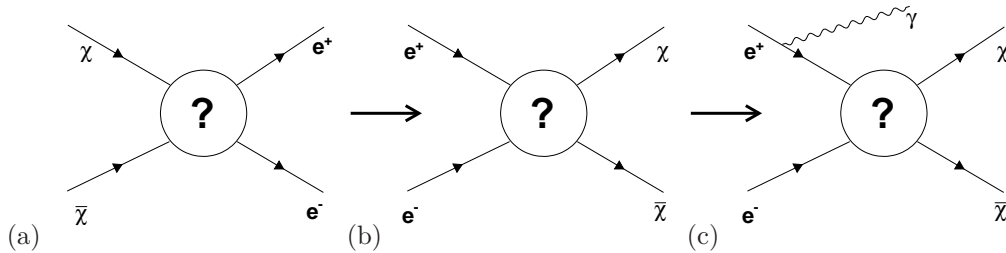


Figure 2: Schematic derivation of the  $e^+e^- \rightarrow \chi\chi\gamma$  production cross section. Except for some generic assumptions on the WIMP nature no presumptions on the interactions involved are imposed, indicated with the question marks.

the new particles, but it might as well be the only kinematically allowed process at the ILC. This is the case when only one new particle exists in the energy range of the ILC. In supersymmetric scenarios the other SUSY masses might be just above the production threshold, preventing the production of the LSP via the decay of heavier particles. Without the need for heavier particles to be produced, ISR searches extend the ILC reach on WIMP masses to  $M_\chi \leq 250$  GeV, just below half the CMS energy. A model independent description of ISR associated WIMP pair production can be derived as in [2]. Under the assumption of only one new particle responsible for the CDM the annihilation cross section of a WIMP pair into an  $e^+e^-$  pair can be estimated from the observed DM relic density (Fig. 2(a)). Exploitation of crossing symmetry yields the cross section for the inverse process (Fig. 2(b)). For soft or collinear photons, factorization theorems can be applied to get the observable signal process depicted in Figure 2(c). It can be shown that the soft/collinear approximation holds also for photons with larger polar angles [2]. The resulting differential production cross section as a function of the emitted photon energy is given by:

$$\frac{d\sigma}{dx} \sim \kappa_e(P_e, P_p) 2^{2J_0} (2S_\chi + 1)^2 \left(1 - \frac{4M_\chi^2}{(1-x)s}\right)^{1/2+J_0}. \quad (1)$$

where  $x = 2E_\gamma/\sqrt{s}$  and  $\kappa_e(P_e, P_p)$  is the polarization dependent squared coupling to the electrons in the initial state. The parameter  $J_0$  is the angular momentum of the dominant partial wave in the production process. Depending on the nature of the interaction  $J_0$  is related to the spin of the exchange particle. Since all known models predict either s-wave ( $J_0 = 0$ ) and p-wave ( $J_0 = 1$ ) WIMP annihilation only these cases are considered here. Figure 3 show the cross section as function of the recoil mass  $M_{recoil}^2 = s - 2\sqrt{s}E_\gamma$  for (a) WIMP masses of 120, 160 and 200 GeV and (b) for a 200 GeV WIMP with  $J_0 = 0$  and  $J_0 = 1$ . The cut-off in the spectrum is related to the WIMP mass and the shape at the threshold provides information on the partial wave quantum number. In order to measure the energy cut-off and the shape, a very good energy resolution for photon detection is demanded from the detector and the reconstruction algorithms.

This analysis is performed with a full simulation of the International Large Detector concept (ILD) [3]. A quadrant of the ILD is shown in Figure 1. The ILC's capability of delivering polarized beams can be used to significantly suppress SM backgrounds, and increase possible signals depending of the structure of the involved interactions. The role of beam polarization at the ILC is discussed in [4].

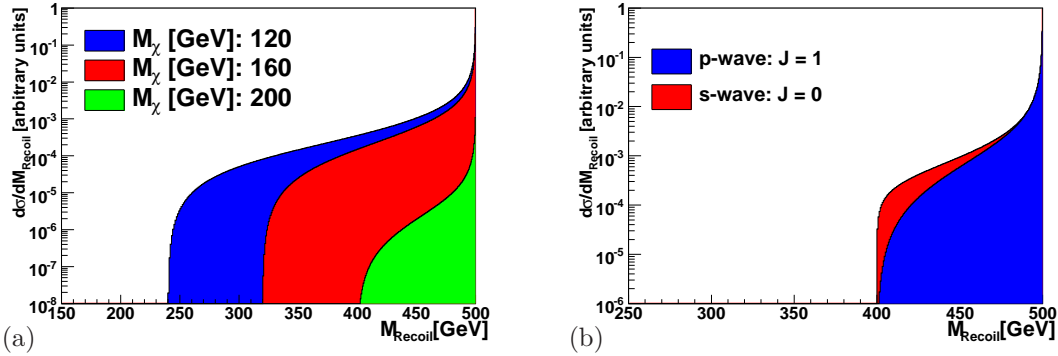


Figure 3: Differential  $\chi\chi\gamma$  production cross section in terms of the recoil mass for (a) different WIMP masses and (b)  $J_0 = 0$  and  $J_0 = 1$  (in arbitrary units).

## 2 ILD detector simulation and photon reconstruction

Single photon events provide the means for a fast validation of the detector model's implementation in the simulation framework. Some key parameters like the overall material budget and the intrinsic energy resolution of the calorimetric system for electromagnetic processes can be determined from the analysis of a large simulated sample of photons shot randomly into the detector. Secondly some aspects of the employed reconstruction algorithms can be studied using single photon events, for example the quality of pattern recognition for electromagnetic clusters, addressed in Subsec. 2.2.

### 2.1 Material budget

A good understanding of the material budget is important for the evaluation of the systematic effects from photon conversions on the event reconstruction. The angular dependence of the material budget that particles originating from the interaction point are exposed to on their way out through the tracking subsystems (vertex detector, TPC, intermediate trackers and support structures) can be evaluated in the detector simulation by counting the number  $N_{gen}$  of photons generated and the number  $N_{unconv.}$  of photons not converted before reaching the ECAL face. The required information is given in the output of the MOKKA implementation of the

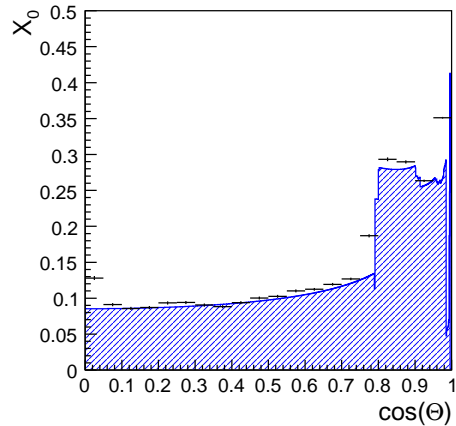


Figure 4: The material budget of the MOKKA implementation of the ILD00 detector model tracking system in terms of the radiation length  $X_0$  as a function of the polar angle  $\Theta$ . For comparison the budget as described in the LoI [3] is plotted in the blue histogram.

ILD00. The material budget in terms of the radiation length is given by:

$$\frac{x}{X_0} = -\frac{9}{7} \ln \left( \frac{N_{unconv.}}{N_{gen}} \right) \quad (2)$$

Figure 4 shows the amount of material determined for the ILD00 detector model implemented in MOKKA v-06-07-p01. The results are based on  $10^6$  single photon events from the SM  $\nu\nu\gamma$  process. For reference the material budget for the tracking system as quoted in the ILD LoI [3] is shown in the underlying histogram. The two most visible features are the increased amount of material at  $\cos \Theta \simeq 0.0$  which is due to the dividing central cathode in the TPC, and the additional material  $\cos \Theta \geq 0.8$  in the forward region is related to the TPC endplate.

## 2.2 Photon reconstruction

The PFLOW paradigm requires that every particle partaking in an event is to be reconstructed individually. For single photon searches especially the performance of the reconstruction algorithms in finding electromagnetic clusters in the ECAL is required to be very good. Figure 5 depicts the average ratio  $N_{rec}/N_{gen}$  of reconstructed photon candidates per generated photon as a function of the generated photon energy (a) and generated photon polar angle  $\cos(\Theta)$  (b). For event reconstruction the MARLIN framework v00-10-04 and the PANDORAPFLOW [5] algorithm v-03-01 have been used. A photon is considered as reconstructed when a PFLOW photon object is found within 0.1 rad (seen from the IP) from a generated one. Additionally the photon object is required to be related to the generated photon on MC level. The ratio continuously rises from one at low photon energies to about three at  $E_\gamma = 250$  GeV. The angular dependence displays a steep rise at polar angles of  $\cos \Theta \simeq 0.8$ . This angular region corresponds to the insensitive region between the ECAL barrel and ECAL endcap where pattern recognition is difficult due to the complex geometry (see Fig. 1). For the analysis presented in the next section this effect is countered by combining the “split” photon clusters into higher level photon objects. Photon clusters that are less apart than 0.04 rad are considered as being fractured remnants from a single incident photon. The result of the merging procedure is shown in Figure 6, where the ratio deviates from unity on the sub-percentage level.

## 3 Determination of WIMP parameters

WIMP production with associated ISR leads to an excess in the photon spectrum at energies below

$$E_\gamma^{max} = \frac{E_b^2 - M_\chi^2}{E_b}. \quad (3)$$

The cross sections are in the order of a few fb, depending on the values of the model parameters  $\kappa_e(P_e, P_p)$ ,  $J_0$ ,  $M_\chi$  and the WIMP spin  $S_\chi$ , resulting in an  $S/B$  ratio of  $10^{-2}$  –  $10^{-3}$  to the irreducible  $\nu\nu\gamma$  background. The parameter  $\kappa_e(P_e, P_p)$  can be deconstructed according to the four possible  $e^+e^-$  helicity configurations:

$$\begin{aligned} \kappa_e(P_e, P_p) = & \frac{1}{4}(1 + P_e)[(1 + P_p)\kappa(e_{RPL}) + (1 - P_{e^+})\kappa(e_{RPR})] \\ & + \frac{1}{4}(1 - P_e)[(1 + P_p)\kappa(e_{LPL}) + (1 - P_{e^+})\kappa(e_{LPR})] \end{aligned} \quad (4)$$

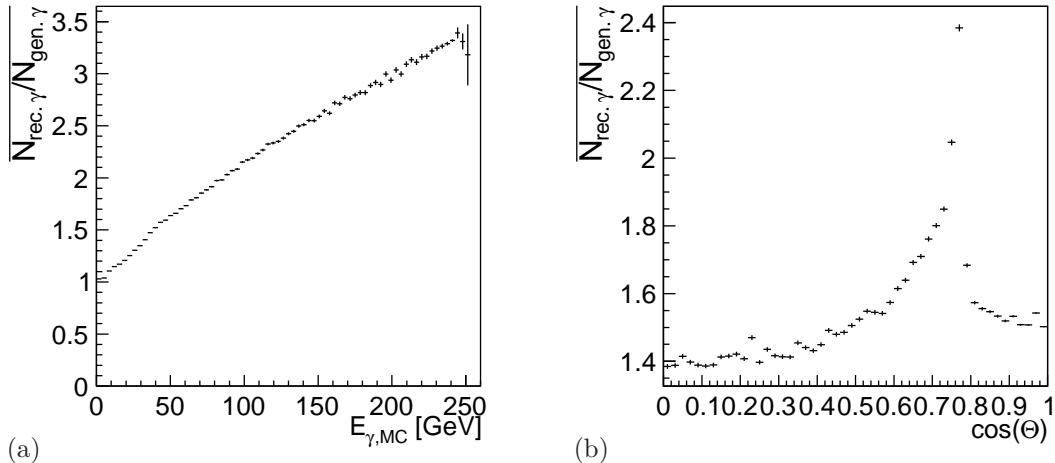


Figure 5: Performance of the photon reconstruction in terms of the ratio  $\overline{N_{rec}/N_{gen}}$  of reconstructed per generated photons as function of photon energy (a) and polar angle (b).

The WIMPs might couple only to right-handed electrons and left-handed positrons ( $\kappa(e_R, p_L)$ , helicity conserving). The couplings might in addition also conserve parity ( $\kappa(e_R, p_L) = \kappa(e_L, p_R)$ ). In both cases the  $S/B$  ratio can be enhanced using polarized beams. The results presented here are based on the full SM  $\nu\nu\gamma(N)\gamma$  ( $N = 0, 1, 2$ ) background simulated for the ILD00 detector model implemented in MOKKA v-06-07-p01. For event generation the WHIZARD event generator [6] is used. Event reconstruction is done within the MARLIN framework v00-10-04 using the PANDORAPFLOW algorithm v-03-01. Each event contains up to two additional ISR photons from the electron and positron. In total an integrated luminosity of  $\mathcal{L} = 250 \text{ fb}^{-1}$  is generated and simulated. The signal itself is not generated and simulated, but is obtained by assignment of weights to the dominant  $\nu\nu\gamma$  background, where the weights are given by the ratio of the cross sections for neutrino and WIMP pair production,  $w = \sigma_{\chi\chi\gamma}/\sigma_{\nu\nu\gamma}$  evaluated for  $E_\gamma$  and  $\Theta$  of the detected ISR photon. For the signal to be statistically independent of the background only half of the simulated SM background is used for the weighted signal, while the other half serves as signal free background. An additional weight is assigned to each event to adjust for the demanded luminosity. The event selection requires a single photon in the detector and no activity in the tracking system.

### 3.1 $2\sigma$ reach on $\kappa$

The reach on  $2\sigma$  level of the ILC on the parameter  $\kappa$  as function of the WIMP mass is shown in Figure 7(a). The plot corresponds to an integrated luminosity of  $200 \text{ fb}^{-1}$ . The WIMP parameters are chosen as  $S = 0$ ,  $J_0 = 1$  and the WIMP couplings to electrons conserve helicity and parity. The contour lines give the reach on the parameter  $\kappa$  as a function of the WIMP mass. The area above the curves is accessible. For each WIMP mass a signal region is defined in the energy distribution of the emitted photons,  $E_{min} \leq E_\gamma \leq E_{max}$ . The lower cut on the photon energies ensures that the recoiling WIMP system is non-relativistic. This

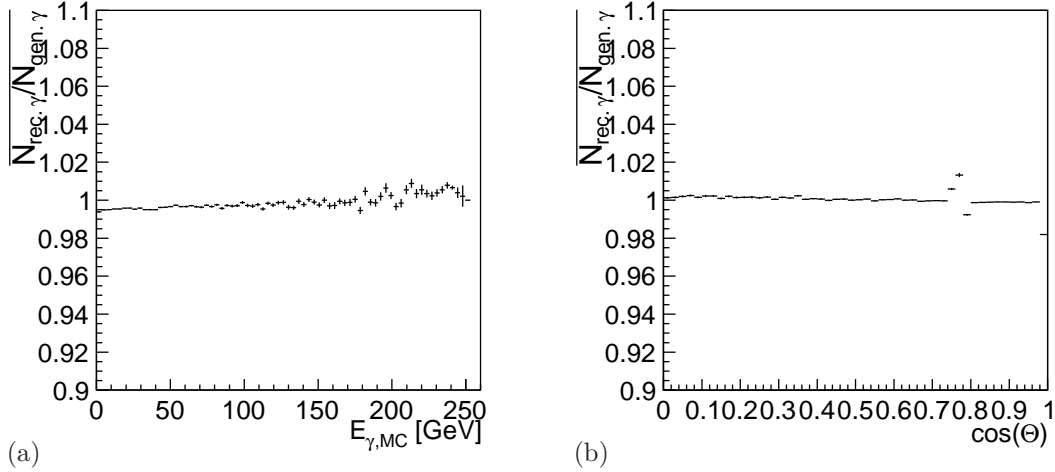


Figure 6: Ratio of  $\overline{N_{rec}/N_{gen}}$  for photons after merging of fractured photon objects.

has to be enforced since only s-wave and p-wave production is assumed. The upper cut is given by the kinematic limit (Eq. 3). This cut serves to increase the signal to background ratio. The result is plotted for different beam polarizations:

- $(P_e/P_p) = (0.0/0.0)$  (red, solid)
- $(P_e/P_p) = (0.8/0.0)$  (blue, wide dashed)
- $(P_e/P_p) = (0.8/-0.3)$  (green, dashed)
- $(P_e/P_p) = (0.8/-0.6)$  (black, dotted)

In this scenario and the given luminosity, no value of  $\kappa$  is accessible for unpolarized beams, hence no WIMP signal can be distinguished from the SM background on  $2\sigma$  level (the corresponding contour line coincides with  $\kappa = 1$ ). With increasing beam polarization the reach is extended for WIMP masses between 160 and 200 GeV down to values of 0.6. The loss of sensitivity to higher masses is due to the kinematic limit, while for lower masses the signal is increasingly reduced by the lower cut on the photon energies. Figure 7(b) shows the reach for the case where the WIMPs ( $S = 1, J_0 = 1$ ), couple only to right handed electrons and left handed positrons. Even for unpolarized beams the reach covers large areas of the  $M - \kappa$  plane for masses up to 200 GeV. With increasing beam polarizations the SM background is suppressed and the signal enhanced, resulting in a large increase of accessible values down to  $\kappa \leq 0.1$ .

### 3.2 Mass measurement

This section on the WIMP mass measurement refers to results from 2007 [7]. The simulated detector model is LDCPrime\_02Sc. The mass of a WIMP candidate can be determined by comparing the signal spectrum to template spectra of different WIMP mass hypotheses

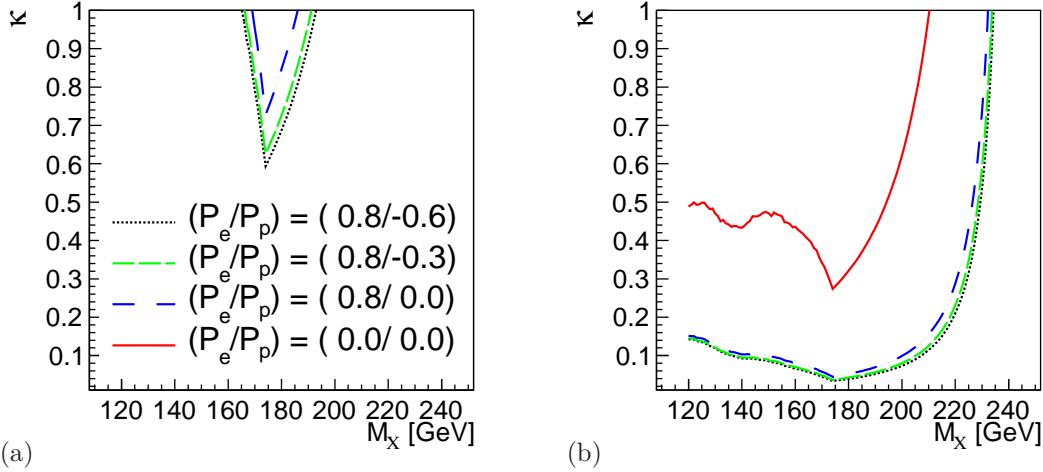


Figure 7:  $2\sigma$  reach for  $200 \text{ fb}^{-1}$  on  $\kappa_e(P_e, P_p)$  as function of the WIMP mass. The results are given for (a) spin 0 WIMPs with helicity and parity conserving couplings and (b) spin 1 WIMPs with couplings conserving only helicity. The contour lines are given for several beam polarizations, see text.

but with otherwise identical parameters. Figure 8(a) shows the  $\chi^2$  for the template fits as a function of the template mass. The signal is a 180 GeV spin 1 WIMP with couplings conserving helicity and parity. The other parameters are set to  $\kappa = 0.3$  and  $J_0 = 1$ . The simulated data is equivalent to an integrated luminosity of  $500 \text{ fb}^{-1}$ . Three different polarization configurations are considered:

- $(P_e/P_p) = (0.0/0.0)$  (solid)
- $(P_e/P_p) = (0.8/0.0)$  (dotted)
- $(P_e/P_p) = (0.8/-0.6)$  (dashed)

Depending on the beam polarization the mass can be determined to:

- $M = 181.5 \pm 3.0 \text{ GeV}$  ( $(P_e/P_p) = (0.0/0.0)$ )
- $M = 180.5 \pm 0.5 \text{ GeV}$  ( $(P_e/P_p) = (0.8/-0.6)$ )

In this case due to the preferable choice of the WIMP couplings highly polarized beams increase the mass resolution by a factor of six.

### 3.3 Simultaneous determination of mass and $J_0$

As pointed out in Section 1 the shape of the photon distribution at the threshold provides information on the dominant partial wave of the production process. The energy distribution of ISR photons from the SM background and the WIMP production can be fitted with the WIMP cross section of formula 1, leaving the WIMP mass and the partial wave  $J_0$  as free

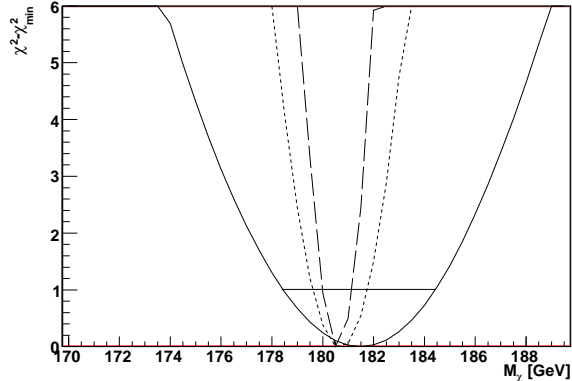


Figure 8:  $\chi^2$  of comparison of 180 GeV spin 1 WIMP ( $\kappa = 0.3, J_0 = 1$ ) signal distribution with signal mass templates for three different polarization configurations, as explained in the text.

parameters in the fit. For  $\mathcal{L} = 100 \text{ fb}^{-1}$  ( $(P_e/P_p) = (0.8/-0.6)$ ) this method recovers a WIMP mass of  $M_\chi = 173.8 \pm 5.1 \text{ GeV}$  and  $J_0 = 1.26 \pm 0.34$  for input parameters of  $M_\chi = 180 \text{ GeV}$  and  $J_0 = 1$  respectively. The remaining input parameters are  $\kappa = 1.0$ ,  $S = 1$  and the couplings conserve helicity only. Although the luminosity is low compared with the ILC design, the s-wave production can be excluded on  $3\sigma$  level, due to the assumed WIMP couplings and beam polarization. The simultaneous mass fit performs significantly worse than the dedicated template fit of the previous section. Since the mass can be determined independently from  $J_0$ , a constraint could be imposed on it in the simultaneous fit. The expected improvement on the  $J_0$  measurement has to be quantified.

## 4 Conclusions

The study presented here shows that there is a good chance of a model independent detection of WIMPs at the ILC. If the WIMP couplings to electrons are not too small, their masses can be measured on the percentage level. Both the detection sensitivity and the mass resolution is enhanced when polarized beams are assumed. First results indicate that even the more involved measurement of the partial wave quantum number seems to be possible, given a good understanding of the SM background.

## 5 Acknowledgments

The authors acknowledge the support by DFG grant Li 1560/1-1.



## 6 Bibliography

### References

- [1] J. Brau *et al.* [ILC Collaboration], *International Linear Collider reference design report. 1: Executive summary. 2: Physics at the ILC. 3: Accelerator. 4: Detectors.*
- [2] A. Birkedal, K. Matchev and M. Perelstein, Phys. Rev. D **70** (2004) 077701, [arXiv:hep-ph/0403004]. *Dark matter at colliders: A model-independent approach.*
- [3] T. Abe *et al.* [ILD Concept Group - Linear Collider Collaboration], *The International Large Detector: Letter of Intent.*
- [4] G. A. Moortgat-Pick *et al.*, Phys. Rept. **460**, 131 (2008), [arXiv:hep-ph/0507011]. *The role of polarized positrons and electrons in revealing fundamental interactions at the linear collider.*
- [5] M. A. Thomson, Nucl. Instrum. Meth. A **611** (2009) 25, [arXiv:0907.3577 [physics.ins-det]]. *Particle Flow Calorimetry and the PandoraPFA Algorithm.*
- [6] W. Kilian, T. Ohl and J. Reuter, *WHIZARD: Simulating Multi-Particle Processes at LHC and ILC*, arXiv:0708.4233 [hep-ph].
- [7] C. Bartels and J. List, arXiv:0901.4890 [hep-ex]. *WIMP Searches at the ILC using a model-independent Approach.* arXiv:0901.4890 [hep-ex].